Molecular Dynamics Simulation Study on Adsorption and Diffusion Processes of a Hydrophilic Chain on a Hydrophobic Surface

Xiao-Lin Wang, Zhong-Yuan Lu,* Ze-Sheng Li,* and Chia-Chung Sun

State Key Laboratory of Theoretical and Computational Chemistry, Institute of Theoretical Chemistry, Jilin University, Changchun 130023, China

Received: June 9, 2005; In Final Form: July 18, 2005

Molecular dynamics simulations are applied to investigate the adsorption and diffusion processes of a single hydrophilic poly(vinyl alcohol) (PVA) chain with different chain lengths on a hydrophobic graphite surface. It is expected that the chain and the surface "dislike" each other because one is hydrophilic and the other is hydrophobic. But surprisingly, a short PVA chain is well adsorbed on the surface, accompanied by large changes in the chain configuration. With increasing degree of polymerization (N), the chain turns gradually from two-dimensional adsorption to possessing certain height in the direction perpendicular to the surface. Moreover, the adsorption energy increases and the diffusion coefficient decreases with increasing N. In particular, for $N = 20$ in equilibrium, the hydroxyls of this short chain are close to the graphite surface in the stable adsorption configuration. In addition, we change the effective dielectric constant to 76.0 to mimic good solvent condition. The chain configurations and the diffusion coefficients both vary in contrast to the foregoing results.

1. Introduction

In three dimensions, polymer dynamics exhibits rich and complex behavior which depends on the solvent conditions and polymer concentration.[1,2] That the dynamics of polymer chains at and near solid interfaces differs profoundly from that in the bulk is intuitively expected. Polymer adsorption on the surface is of technological and scientific importance in the field of colloids and biomolecules. Examples include the two-dimensional (2-D) diffusion of DNA oligonucleotides confined to biological interfaces such as cell membranes.[3,4] The diffusion of confined polymers at surface is always a fundamental, yet problematical topic in polymer physics.[1,2,5−8] It has attracted attention for decades already.

Computer simulations for the mechanism of a single polymer chain adsorbed and diffusing on a surface are important, as experimental studies on an isolated polymer chain are difficult in most cases. Many simulations had been performed for different polymeric systems with multiple chains (or a single chain) adsorbing and diffusing on the surface.[9−13]

Granick and co-workers studied poly(ethylene glycol) molecules adsorbed on solid surface by means of fluorescence microscopy.[14−17] They found that the diffusion coefficient (D) of such chains scales with the degree of polymerization (N) as $N^{-3/2}$, which is characteristic for 2-D chain models. On the other hand, Maier and Rädler found much weaker scaling, namely N^{-1}, when studying adsorbed DNA in a lipid bilayer.[3,4] In the simulations, Milchev and Binder[12] showed that D scales with the chain length as $N^{-1.1}$; Azuma and Takayama[9] obtained $D \sim N^{-3/2}$; but Falck et al.[10] found that D should scale as N^0. Therefore, the dynamics behavior of a confined polymer on a surface is still an interesting research topic.

In this research, our main objective is to study the adsorption and diffusion processes of a hydrophilic chain on a hydrophobic surface. The similar hydrophilic−hydrophobic system usually appears in the coating industry, such as drawing the paint on different surfaces. Moreover, wetting, surface adhesion, and flow in confined geometries are examples of such systems. Recently, Willett et al. have investigated different adhesion interactions of amino acids to inorganic surfaces showing possible applications on biodetection.[18] Therefore, the results of this paper may be helpful for further understanding of the configuration change and the dynamics of the hydrophilic polymer chain adsorbed on a hydrophobic surface.

We consider a single PVA chain adsorbed on the rigid (001) graphite surface in a vacuum and in mimetic good solvent condition. The adsorption and diffusion processes of the chain are investigated through energy minimizations and molecular dynamics simulations with all the molecular degrees of freedom being taken into account. Only one single chain is adopted in a simulation because it relates directly to 2-D polymer diffusion in very dilute solution. In addition, PVA is a widely available hydrophilic material, comes in a range of molecular weights, and is easy to use. The hydrophobic graphite surface is chosen because of its relative simplicity and rigidity, so that it can be treated as a fully rigid body for our purposes. We follow a two-step strategy: (i) first we carry out direct energy minimizations of the PVA chain close to the graphite surface with different initial configurations in order to relax the model; (ii) then we use the most stable configuration after minimization to perform MD simulations. In the theory of dynamical scaling the two key quantities are the radius of gyration (R_g) and the center-of-mass diffusion coefficient D of the chain. We thus use them to describe the characteristics for the system in this paper. Interestingly we find that, for $N = 20$ in equilibrium, the hydroxyls of this short chain are close to the hydrophobic surface in the stable adsorption configuration. We also change the effective dielectric constant to 76.0 to mimic good solvent condition. The results are compared with the systems in a vacuum (which can be taken as in bad solvent condition). The

* To whom correspondence should be addressed. E-mail: luzhy@mail.jlu.edu.cn. (Z.-Y.L.); zeshengli@mail.jlu.edu.cn (Z.-S.L.).

10.1021/jp053116w CCC: $30.25
Published on Web 08/25/2005

chain configurations and the diffusion coefficients both vary greatly, showing strong dependence on the solvent condition.

2. Models and Simulation Details

The MD simulation is carried out in a box with 3-D periodic boundary conditions. The PVA chain is embedded into the simulation box with a fixed (001) graphite surface parallel to the *XY* plane. We choose *N* for the chain as 20, 30, 50, 60, and 80, respectively. The thickness of the surface is around 15 Å with 4 layers. The length of the simulation box in the *Z* direction is 80 Å, which is large enough so that the interactions between the adsorbed PVA chain and the periodic images of graphite in the top plane can be ignored. In this way, the 3-D periodicity inherent in the model is transformed into an actual 2-D periodicity thus simulating an infinitely extended surface.

A high-quality force field COMPASS (condensed-phase optimized molecular potentials for atomistic simulation studies)[19−21] is adopted in the simulation. In contrast to early force fields which were mostly parametrized based on gas-phase data or ab initio calculations, COMPASS combines ab initio and empirical parametrization procedures. In addition, it adds cross terms to potential in order to consider the influence of all atoms close-by for distortions of bond length or bond angle. It enables accurate and simultaneous prediction of structural, conformational, vibrational, and thermophysical properties for a broad range of molecules in isolation and in condensed phases. The energy calculation with COMPASS is a combination of bonding and nonbonding terms. The bonding terms include stretching, bending, and torsion energy as well as the diagonal and off-diagonal cross coupling terms. The van der Waals interactions are truncated at $r_c = 12$ Å by using a spline function from 11 Å. The Coulomb interactions are calculated via Ewald summation.[22] Since the graphite atoms do not possess partial charges, the interactions between the PVA chain and the surface are simply van der Waals type. However, the intramolecular Coulomb interactions of the PVA chain must be treated via Ewald summation instead of the cutoff method, so that the intrachain and the chain−surface interactions can be studied with similar accuracy. Before the MD simulations, energy minimizations are performed to relax the local unfavorable structure of the chain. Subsequently, MD simulations with 5 ns are performed under NVT thermodynamics ensemble. Every simulation is performed three times to ensure the reliability of the results. The equations of motion are integrated with a time step of 1 fs. The constant temperature $T = 300$ K is controlled through the Berendsen thermostat[23] with a relaxation time of 0.1 ps.

In these simulation runs, the total and potential energies show an initial decrease, possibly with a few separate kinetic stages, and then fluctuate around a constant value, indicating the achievement of the equilibrium state. This process corresponds to the adsorption and diffusion dynamics of the PVA chain from the initial configuration. We then change the dielectric constant to 76.0 to mimic the good solvent condition. Of course in this way the explicit solvation effects cannot be considered. Nevertheless, we can directly study the effects by simply changing the bad to the good solvent condition on the chain configurations and dynamics.

3. Simulation Results and Discussion

In this section, we show the simulation results, such as the chain configurations, the diffusion coefficient, the adsorption energy, and the bond orientational order parameter. All simulations are run until the chain reaches its equilibrium structure,

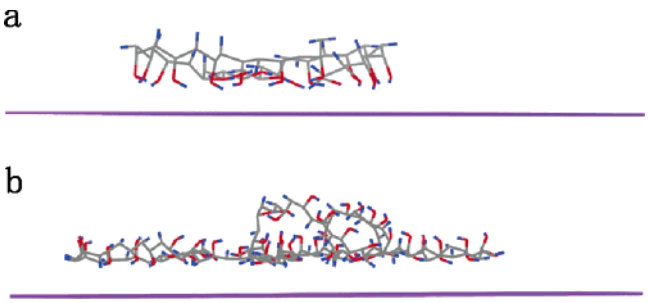

Figure 1. Snapshots for PVA chains adsorbed on the graphite surface with $N = 20$ and 60 are displayed in panels a and b, respectively. The blue color denotes hydrogen and the red denotes oxygen. Only one graphite layer is shown in the side view. The other three graphite layers and the simulation box boundary are not shown for clarity.

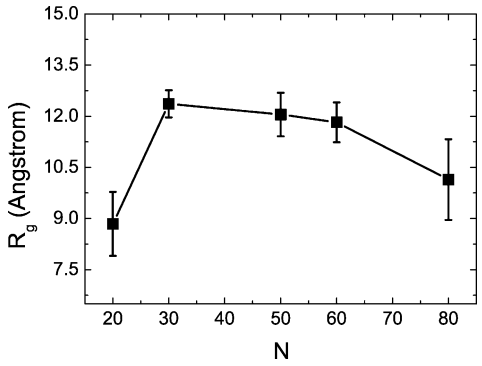

Figure 2. The mean radius of gyration R_g vs the chain length *N*. The symbols are MD simulation results. The error bars are the standard deviation measured in three parallel simulations.

i.e., until the simulated chain lost its memory of the initial configuration, and running the program further results in no discernible changes in the structural properties and energy beyond natural fluctuations.

3.1. In a Vacuum (or Bad Solvent). *3.1.1. Configuration Change of PVA during Adsorption.* In Figure 1 we show the simulation snapshots of the PVA chains with two typical *N* in equilibrium. Figure 1a is for $N = 20$, showing good adsorption of this short PVA chain on the hydrophobic surface. Interestingly, the hydroxyls of the chain are all close to the surface in the equilibrium states. This will be discussed further below. Figure 1b is for $N = 60$, which shows apparent partial desorption of the PVA chain.

With time evolution, the chain configuration changes from initially isolated "random-coil" in a vacuum to a compact form adsorbed on the surface. In the first several hundred picoseconds, chain adsorption occurs accompanied by diffusion. When the energy dynamically reaches constant, the chain dynamics is mainly dominated by the diffusion process. To show the chain configuration change during the adsorption, we calculate the mean radius of gyration which is defined as

$$\langle R_g \rangle = \sqrt{\left\langle \frac{1}{N}\sum_{i=1}^{N} (\mathbf{r}_i - \mathbf{r}_{cm})^2 \right\rangle} \qquad (1)$$

where $\mathbf{r}_i$ and $\mathbf{r}_{cm}$ denote the position vector of each atom in a chain and the center-of-mass for the whole chain, respectively. Figure 2 shows the change of calculated $\langle R_g \rangle$ with increasing *N*. Apparently, R_g first increases, then decreases, and the maximum corresponds to $N = 30$. By seeing the simulation snapshots, one can find that the PVA chain containing 20 or

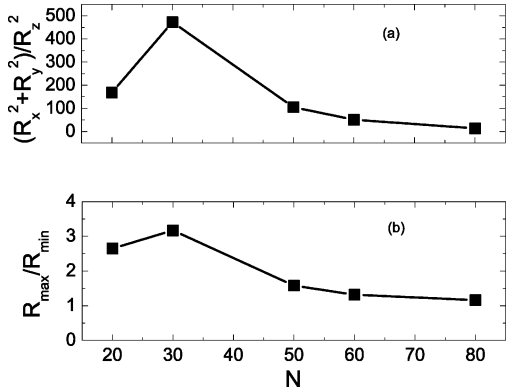

Figure 3. These two ratios are calculated from the three principal components of R_g. Panel a shows the ratio of $(R_x^2 + R_y^2)/R_z^2$ vs N and panel b shows the ratio of R_{max}/R_{min} vs N, where R_{max} denotes the larger one of R_x or R_y, and R_{min} denotes the other.

30 monomers is ultimately well-adsorbed on the graphite surface with a 2-D configuration. The polymer comprised of 30 monomers is therefore occupying a larger area on the surface than that of 20 monomers, resulting in a bigger R_g for $N = 30$. It appears certain height along the Z axis for the PVA chain adsorbed on the surface while further increasing the chain length over 30. In these cases, the chains do not entirely spread, and the adsorption is not strong.

For the sake of characterizing the anisotropic configuration of the polymer and interpreting the configuration change during adsorption, we calculate two ratios such as $(R_x^2 + R_y^2)/R_z^2$ and R_{max}/R_{min}. R_x, R_y, and R_z are the components in three principal directions of R_g. R_{max} and R_{min} correspond to the large and small magnitude between R_x and R_y, respectively. The results are shown in Figure 3, parts a and b. Both ratios have the same tendency that the values first increase then decrease with increasing N. The turning point also corresponds to $N = 30$. This is consistent with the result of R_g as shown in Figure 2.

The component of R_g along the Z axis that is perpendicular to the surface is strongly reduced during the adsorption. The components of R_g along the X and Y axes display significant increases due to the chain spreading on the surface. The short chains with $N = 20$ or 30 are well adsorbed on the surface and therefore present 2-D configurations. Thus R_x and R_y are larger and R_z is very small in these two cases. As for $N = 50$, 60, and 80, the above ratios decrease with increasing N. Although the chains change the configurations during the adsorption, in these cases they still partially keep the initial "random-coil" configuration. This is due to the competition between the intramolecular and the chain−surface interactions, which brings on an increase of R_z with increasing N. The intramolecular interaction, consisting of the van der Waals, the electrostatic, and the hydrogen bond interactions, turns out to be larger with high N, thus the adsorbed chains are more isotropic in space.

3.1.2. Diffusion of PVA Chain on the Surface. After the adsorption process, which is monitored by the interaction energy between the chain and the surface starting to fluctuate only around a constant value, the dynamics of PVA is mainly dominated by the chain diffusion on the surface. We calculate the diffusion coefficients of the chains via the Einstein relation. Figure 4 shows the change of D with varying degree of polymerization. It is clear that D decreases greatly as N increases from 20 to 80. However, there is no apparent scaling between D and N, which may be due to the comparatively short chain lengths in our model. The dependence of D on N can be explained by the change of interaction energy between the chain

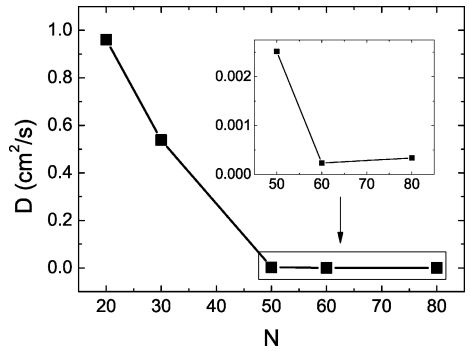

Figure 4. Diffusion coefficients, D, are plotted against degree of polymerization of the PVA chain, N.

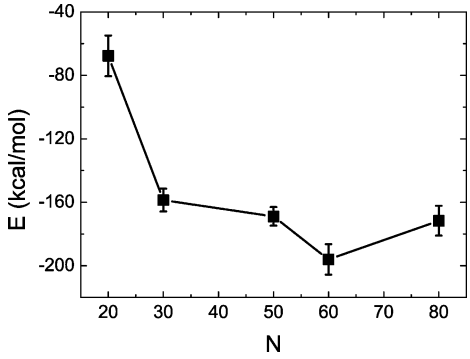

Figure 5. Adsorption energy E vs chain length N.

and surface with increasing N. This adsorption energy can be calculated via

$$E_{int} = E_{tot} - (E_{frozen} + E_{plane}) \quad (2)$$

where E_{tot} is the potential energy of the chain plus the surface system in equilibrium, E_{frozen} is the potential energy of the adsorbed chain isolated in a vacuum with the geometry unchanged, and E_{plane} is the potential energy of the surface. Larger molecular configuration deformation allows for better adsorption of the chain onto the surface; however, this will break the intramolecular hydrogen bonds which causes a free energy penalty. Therefore such an interaction competition results in a limit of the adsorption energy with increasing N, which can be seen in Figure 5. There is an increment of the adsorption energy with increasing degree of polymerization. The limit value is around −158.60 kcal/mol, starting from $N = 30$. The change from −67.70 kcal/mol for $N = 20$ to −158.60 kcal/mol for $N = 30$ corresponds to the large decrease of D in Figure 4. Further decrease of D with increasing N from $N = 30$ may be due to the increase of the molecular weight. Larger adsorption energy and higher molecular weight both reduce the diffusion coefficient of PVA on the surface. It should be noted that the adsorption energy of $N = 80$ is smaller than that of $N = 60$. This results in the slight increase of D ($N = 80$) as compared with D ($N = 60$). In the case of $N = 80$, the intramolecular interaction is strong enough to keep the chain configuration mostly as "random-coil", thus decreasing the contact area between the chain and the surface. Correspondingly there is a decrease of adsorption energy whose contribution is purely due to van der Waals.

Changing the simulation box size will influence the value of the calculated diffusion coefficient due to the long-range nature of the inherent hydrodynamic interactions.[24] To see the effects, we choose the shortest chain of 20 monomers to simulate with different box sizes. We increase and decrease the dimension of

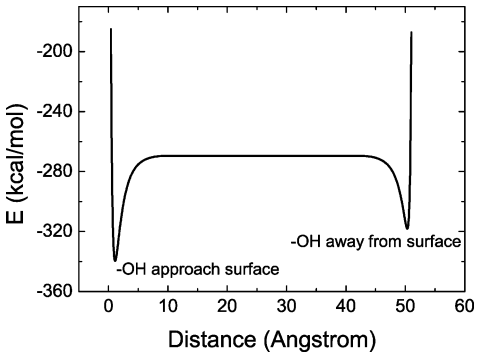

Figure 6. The adsorption energy E of hydroxyls approaching the surface and that of hydroxyls away from the surface. The difference of E for these two adsorption states is 21.62 kcal/mol.

TABLE 1: The Dependence of Calculated Diffusion Coefficient on the Simulation Box Size

box size	diffusion coeff (cm^2/s)
original box size	0.96
17% smaller for each side	0.78
50% larger for each side	1.43

each side by 50% and 17%, respectively, and calculate the diffusion coefficients. The results are presented in Table 1. Comparing the three data, we can see that there is an increment of diffusion coefficient while increasing the box size. Since we have adopted the same box size in the above simulations, there will be more influence on the values of the diffusion coefficients of longer chains. However, from Figure 4 we can see that D decreases largely with changing the chain lengths from shorter ($N = 20$, 30) to longer ($N > 50$). Thus, although the values of the diffusion coefficients for longer chains may be underestimated due to comparatively smaller box size, the tendency of D decreasing with increasing N may not change.

3.1.3. A Special Case: *PVA with $N = 20$.* The behavior of PVA with $N = 20$ is different from that of the other chain lengths from the above discussion. By seeing the snapshots, we find that the hydroxyls of PVA with $N = 20$ are close to the hydrophobic surface in equilibrium states. This is somewhat contradictory to what we have expected that the hydroxyls and the hydrophobic surface should "dislike" each other. Figure 1a shows the snapshot of a stable configuration. To find the reason for this phenomenon, we compare the adsorption energy of hydroxyls approaching the surface with that of hydroxyls away from the surface. Since the simulation is done with 3-D periodic boundary conditions, we can do this by changing the distance between the chain and the surface stepwise. Figure 6 shows that the absolute value of the interaction energy for hydroxyls approaching the surface is 21.62 kcal/mol larger than that for hydroxyls away from the surface. It indicates that the adsorption for the former is stronger, and the chain configuration is more stable. However, when N increases, this phenomenon no longer exists (see, for example, Figure 1b). The hydroxyl bond vectors appear randomly in the system, which is attributed to the strong intramolecular interactions so that the PVA chain prefers to be a "random-coil".

We then calculate the orientational order parameters of C−O and O−H bonds to describe the local bond orientation behavior after adsorption.[25] The order parameters are defined commonly as

$$P_1(z) = \langle \cos(\theta) \rangle \tag{3}$$

$$P_2(z) = 0.5 \times \langle 3 \cos^2(\theta) - 1 \rangle \tag{4}$$

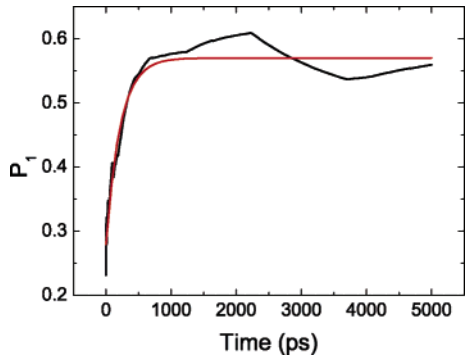

Figure 7. The order parameter $P_1(z) = \langle \cos(\theta) \rangle$ of the bond C−O, where θ is the angle between the vector $\boldsymbol{R}_{CO}(z) = [\mathbf{R}_O - \mathbf{R}_C](z)$ and the Z axis vector $\mathbf{N}_z$. We fit the curve with a first-order exponential decay function as $P_1 = y_0 + A_1 \exp(-x/t_1)$. The characteristic decay time t_1 is 219.07 ps for $N = 20$.

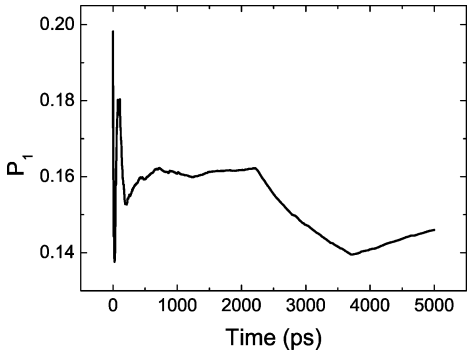

Figure 8. The order parameter $P_1(z) = \langle \cos(\theta) \rangle$ of the bond O−H, where θ is the angle between the vector $\mathbf{R}_{OH}(z) = [\mathbf{R}_H - \mathbf{R}_O](z)$ and the Z axis vector $\mathbf{N}_z$.

where θ is the angle between the specific bond vector and the Z axis vector $\mathbf{N}_z$. The order parameter $P_2(z)$ cannot distinguish between "close to" and "away from" orientations of hydroxyls with respect to the surface. We thus have only plotted $P_1(z)$ of C−O and O−H bonds as a function of time by means of cumulative average method. The results are shown in Figures 7 and 8, respectively. There is a distinct orientation for the C−O bond as shown in Figure 7. We fit the curve with the first-order exponential decay function. The standard relaxation time is 219.07 ps for the PVA chain with $N = 20$, which characterizes the time for cooperative C−O bond orientation. The angle between the $\mathbf{R}_{CO}$ vector and $\mathbf{N}_z$ is small, so the direction of the C−O bond is nearly perpendicular to the surface. In other words, the positions of hydroxyls are between the chain backbone C atoms and the graphite surface, i.e., approaching the graphite. But from Figure 8, we can see that the orientation of O−H is almost random. This result can be compared with the cases of small molecules such as water at the extended hydrophobic surface.[26]

3.2. In Good Solvent. We change the dielectric constant to 76.0 to mimic the good solvent condition.[27] Of course in this way the explicit solvation effects cannot be considered. Nevertheless, we can directly study the effects by simply changing the bad to the good solvent condition on the chain configurations and dynamics. For saving time and avoiding repetitious work, we have only chosen two representative chains with different lengths as $N = 20$ and 60.

The PVA chains can be adsorbed onto the hydrophobic surface, showing 2-D configurations, no matter how many monomers the chain contains (20 or 60). The adsorption takes place very fast and the equilibrium is attained after about 5 ps. Sequentially, 2-D chain configurations are always retained in

TABLE 2: The Adsorption Energy *E* and Diffusion Coefficient *D* Calculated in Vacuum and Good Solvent, Respectively, for the PVA Chain with Length *N* as 20 and 60

	N	in a vacuum	in good solvent
E (kcal/mol)	20	−67.70	−73.90
	60	−195.97	−211.38
D (cm^2/s)	20	0.96	0.76
	60	2.34×10^{-4}	2.14×10^{-4}

the successive diffusion process. At last the chain possesses the most stable configuration as one layer on the surface. In such systems, the Coulomb interactions are largely screened by the good solvent. For example, the Coulomb energy value changes from −371.57 to −2.9 kcal/mol for $N = 20$, and from −610.68 to −8.8 kcal/mol for $N = 60$. So the intramolecular interactions are reduced in such cases and dominated mostly by van der Waals, which finally leads to the better adsorption of the chain in good solvent condition than that in a vacuum. Compared to the relative results in a vacuum, we can find that the contact area between the chain and the surface increases, also the interaction energy increases, due to the better 2-D configuration. Consequently, the diffusion coefficient will decrease with increasing interaction energy. The results are shown in Table 2.

In summary, it is clear that solvent effect has an important influence on the configurations and the dynamics of the hydrophilic−hydrophobic system from the discussion above. It can change not only the equilibrium chain configuration after the adsorption, but also the dynamics behavior of the chain on the surface.

4. Conclusions

In the present paper, MD simulations are used to investigate the adsorption and diffusion behavior of a single flexible hydrophilic PVA chain on a hydrophobic graphite surface. Although there should be repulsion between the chain and the surface because of their different characteristics, the PVA chain is still adsorbed well onto the surface and possesses different behavior with increasing chain length.

In a vacuum (or bad solvent), the short PVA chain containing 20 or 30 monomers is well adsorbed onto the hydrophobic surface and displays 2-D configuration, whereas the longer chain containing more than 50 monomers possesses certain adsorption height on the surface. The calculated results of mean radius of gyration and two ratios such as $(R_x^2 + R_y^2)/R_z^2$ and R_{max}/R_{min} manifest the chain length dependence of the adsorption configuration. The adsorption energy increases and accordingly the diffusion coefficient decreases with increasing *N*. The data for *D* do not obey scaling law with $N^{-\nu}$ for the considered chain lengths.[28−31] For $N = 20$, the PVA hydroxyls are close to the hydrophobic surface in adsorption equilibrium. We compare the adsorption energy for hydroxyls approaching the surface with that for hydroxyls being away from the surface, and find that the absolute value for the former is 21.62 kcal/mol larger than that for the latter. It indicates that the adsorption of hydroxyls approaching the surface is stronger, and the configuration is more stable. But when the degree of polymerization increases, there is no preferential orientation of the hydroxyls.

In good solvent, the PVA chain with initial "coil" configuration can be adsorbed very well on the surface and displays 2-D form no matter how many monomers it contains (20 or 60). Moreover, the adsorption speed is very fast. We obtain the changes of adsorption energy and diffusion coefficient due to adding the good solvent in contrast to the values of the chain in a vacuum. The larger adsorption energy determines the smaller diffusion coefficient, which means the slower diffusion rate.

The above results show that a hydrophilic chain can be adsorbed onto the hydrophobic surface. This is strongly affected by the solvent conditions. By changing from the bad to the good solvent, the chain can be better adsorbed, showing a 2-D configuration. Thus by fine-tuning the solvent quality, one can manipulate the behavior of the chain. Also it is possible to change the surface from hydrophobic to hydrophilic if enough hydrophilic chains are adsorbed.

Acknowledgment. This work is supported by the National Science Foundation of China (20490220, 20404005).

References and Notes

(1) de Gennes, P.-G. *Scaling Concepts in Polymer Physics*; Cornell University Press: Ithaca, NY, 1979.
(2) Doi, M.; Edwards, S. F. *The Theory of Polymer Dynamics*; Clarendon Press: Oxford, UK, 1986.
(3) Maier, B.; Rädler, J. O. *Phys. Rev. Lett.* **1999**, *82*, 1911.
(4) Maier, B.; Rädler, J. O. *Macromolecules* **2000**, *33*, 7185.
(5) Yethiraj, A. *Adv. Chem. Phys.* **2002**, *121*, 89.
(6) Sheiko, S. S.; Möller, M. *Chem. Rev.* **2001**, *101*, 4099.
(7) Granick, S. *Eur. Phys. J. E* **2002**, *9*, 421.
(8) Granick, S.; Kumar, S. K.; Amis, E. J.; Antonietti, M.; Balazs, A. C.; Chakraborty, A. K.; Grest, G. S.; Hawker, C.; Janmey, P.; Kramer, E. J.; Nuzzo, R.; Russell, T. P.; Safinya, C. R. *J. Polym. Sci. Part B*: *Polym. Phys.* **2003**, *41*, 2755.
(9) Azuma, R.; Takayama, H. *J. Chem. Phys.* **1999**, *111*, 8666.
(10) Falck, E.; Punkkinen, O.; Vattulainen, I.; Ala-Nissila, T. *Phys. Rev. E* **2003**, *68*, 050102.
(11) Cavallo, A.; Müller, M.; Binder, K. *J. Phys. Chem. B* **2005**, *109*, 6544.
(12) Milchev, A.; Binder, K. *Macromolecules* **1996**, *29*, 343.
(13) Wang, Y.; Mattice, W. L. *Langmuir* **1994**, *10*, 2281.
(14) Sukhishvili, S. A.; Chen, Y.; Müller, J. D.; Gratton, E.; Schweizer, K. S.; Granick, S. *Nature* **2000**, *406*, 146.
(15) Bae, S. C.; Xie, F.; Jeon, S.; Granick, S. *Curr. Opin. Solid State Mater.* **2001**, *5*, 327.
(16) Sukhishvili, S. A.; Chen, Y.; Müller, J. D.; Gratton, E.; Schweizer, K. S.; Granick, S. *Macromolecules* **2002**, *35*, 1776.
(17) Zhao, J.; Granick, S. *J. Am. Chem. Soc.* **2004**, *126*, 6242.
(18) Willett, R. L.; Baldwin, K. W.; West, K. W.; Pfeiffer, L. N. P. *Natl. Acad. Sci. U.S.A.* **2005**, *102*, 7817.
(19) Sun, H. *J. Phys. Chem. B* **1998**, *102*, 7338.
(20) Sun, H.; Ren, P.; Fried, J. R. *Comput. Theor. Polym. Sci.* **1998**, *8*, 229.
(21) Rigby, D.; Sun, H.; Eichinger, B. E. *Polym. Int.* **1997**, *44*, 311.
(22) Allen, M. P.; Tildesley, D. J. *Computer Simulation of Liquids*; Clarendon: Oxford, UK, 1987.
(23) Berendsen, H. J. C.; Postma, J. P. M.; van Gunsteren, W. F.; DiNola, A.; Haak, J. R. *J. Chem. Phys.* **1984**, *81*, 3684.
(24) Yeh, I.-C.; Hummer, G. *J. Phys. Chem. B* **2004**, *108*, 15873.
(25) Jensen, M. ø.; Mouritsen, O. G.; Peters, G. H. *J. Chem. Phys.* **2004**, *120*, 9729.
(26) Lee, C. Y.; McCammon, J. A.; Rossky, P. J. *J. Chem. Phys.* **1984**, *80*, 4448.
(27) Raffaini, G.; Ganazzoli, F. *Langmuir* **2004**, *20*, 3371.
(28) Zimm, B. H. *J. Chem. Phys.* **1956**, *24*, 269.
(29) Rouse, P. E. *J. Chem. Phys.* **1953**, *21*, 1272.
(30) Shannon, S. R.; Choy, T. C. *Phys. Rev. Lett.* **1997**, *79*, 1455.
(31) Ala-Nissila, T.; Herminghaus, S.; Hjelt, T.; Leiderer, P. *Phys. Rev. Lett.* **1996**, *76*, 4003.